Available online at www.sciencedirect.com
ScienceDirect
Journal of the European Ceramic Society 28 (2008) 1649–1655
www.elsevier.com/locate/jeurceramsoc

Improvement of composite sol–gel process for manufacturing 40 μm piezoelectric thick films

A. Bardaine [a,*], P. Boy [a], P. Belleville [a], O. Acher [a], F. Levassort [b]

[a] *Laboratoire Sol–Gel, CEA/Le Ripault, BP 16, 37260 Monts, France*
[b] *Université François Rabelais, LUSSI, 10 boulevard Tonnellé, BP 3223, 37032 Tours Cedex 1, France*

Received 28 May 2007; received in revised form 20 October 2007; accepted 26 October 2007
Available online 15 January 2008

Abstract

In this study, high performance piezoelectric thick films were prepared by depositing only a few sol–gel infiltrated composite layers on $Si/SiO_2/Ti/Pt$ wafers. Lead zirconate titanate (PZT) powder, binder and infiltration sol were synthesised from the same-laboratory made time-stable polymeric PZT sol. Adding coarse powder (50 wt%) to the sol precursor, crack-free coatings were prepared by dip coating in the 30–50 μm thickness range in only 3–6 layers. The results showed that good performance can be achieved by controlling sol concentration, powder charge, composite sol ageing, number of infiltrations and heat treatments. The initial results showed that only a limited number of infiltrations are needed in the final stack to obtain high piezoelectric performance. For instance, a 40 μm thick film was prepared with 6 composite layers with a 0.7 M PZT sol charged with 50 wt% PZT powder after 2 months' ageing. Poling was performed for 5 min under 15 V/μm in an oil bath at 170 °C after 5 infiltrations and final annealing at 700 °C for 10 min in RTA. Despite substrate clamping, this coating reached an effective thickness coupling factor up of to 39% at a resonance frequency of 30 MHz. This result was obtained with a non-doped PZT powder.

Keywords: Sol–gel; Composite; Piezoelectric properties; PZT; Ultrasonic transducers

1. Introduction

Ferroelectric lead zirconate titanate (PZT) is widely used for piezoelectric device applications such as MEMS, actuators and ultrasound transducers. In medical imaging, the exploration of superficial tissues in fields such as dermatology, ophthalmology and microsurgery requires the development of high frequency (40–50 MHz) ultrasound probes. Piezoelectric polymers or copolymers such as PVDF and P(VDF-TrFE) have limited electromechanical performance (k_t∼25%) and lead-based ceramics (k_t∼50%) have also been widely investigated. However, for these materials, working at high frequency requires the preparation of films of few tens of microns thick (for example around 40 μm for a resonance frequency of 30 MHz). To deposit films with such high piezoelectric performance, several processes such as lapping,[1] tape casting,[2] screen printing,[3] sol–gel[4] and inkjet printing[5] have been studied. Sol–gel chemistry has certain advantages among these techniques such as low processing temperatures, low cost equipment, easy stoichiometry and film thickness control. Furthermore, sol–gel chemistry is very appropriate for deposition onto complex shape substrates. PZT sol–gel films, first studied by Fukushima et al.,[6] were developed as thin films for various applications such as non-volatile memories,[7] capacitors[8] and MEMS.[9] To increase film thickness, a sol–gel route using a charged sol, also called a composite sol, was first developed by Barrow et al.[4,10] Using the spin-coating technique, 5–200 μm thick films were prepared with good piezoelectric properties. The best reported results were obtained using 1–2 μm thick single layers, since authors reported that increasing the single layer thickness leads to a degradation of film density and piezoelectric properties.[11] Other studies showed that coating infiltrations with a PZT sol improved both densification and surface roughness and led to enhancement of the piezoelectric coefficient d_{33}.[12,13] Infiltration is usually performed after deposition of each composite layer.[14]

In the study reported here, the sol–gel composite process was used to prepare dip-coated PZT thick films deposited on $Si/SiO_2/Ti/Pt$ wafers. The piezoelectric and electromechanical properties were mainly studied by measuring the effective

* Corresponding author.
E-mail addresses: anthony.bardaine@cea.fr (A. Bardaine), philippe.boy@cea.fr (P. Boy).

0955-2219/$ – see front matter © 2007 Elsevier Ltd. All rights reserved.
doi:10.1016/j.jeurceramsoc.2007.10.014

thickness coupling factor k_t which is a determining parameter for ultrasound transducer applications. 40 μm thick films were prepared to make high frequency ultrasonic transducers at 30–40 MHz.

We used a very stable high viscosity PZT polymeric sol as a binder. It was first optimised to prepare reproducible thin film capacitance.[15] Unlike most studies which mixed commercial PZT powder in the composite slurry, the powder here was synthesised from the PZT polymeric sol, and better chemical homogeneity was therefore expected.

This study also investigated the ability of the process to obtain thick films in a limited number of composite layers. Films were prepared and optimised using 5–10 μm thick single layers. To obtain the appropriate thickness and properties, binder concentration, powder content and variation in film thickness with sol ageing were taken into account.

The influence of heat treatment on thick film performance (in particular the k_t) was also investigated and showed the benefit of short heat treatments.

Finally, infiltrations were processed to avoid voltage breakdown and allow high voltage polarisation. Infiltrations were only processed after the last composite layer, preserving the porous structure at the film/substrate interface.[16] Piezoelectric performance was also improved by limiting the number of infiltrations.

In Section 2, each step of the composite sol preparation and PZT film development is described. Structural and electromechanical results are discussed in Section 3.

2. Experimental details

2.1. PZT sol synthesis

Using ethylene–glycol and *n*-propanol as solvents, the $Pb(Zr_{0.52}Ti_{0.48})O_3$ sol[15] was synthesised with lead acetate trihydrate (Normapur), zirconium *n*-propoxide at 70% in *n*-propanol (Fluka) and titanium isopropoxide (Aldrich) as precursors. An excess of 10% lead was introduced in the sol to compensate for the removal of PbO during the annealing process. The synthesis is depicted in Fig. 1. A solution with a viscosity of 33.5 cP was obtained for a concentration of 20 wt% PZT (0.7 M). This solution was used as binder in the composite slurry and as infiltration sol.

2.2. Powder synthesis

The powder charge was prepared from the previous sol in 4 steps: gelification, solvent release, calcination and densification. The PZT sol was mixed with a basic solution of NH_4OH at pH 11, then placed in the oven for 30 min at 80 °C for gelification. The gel was heat treated for 6 h at 200 °C to remove the solvents. The yellow solid material obtained was crushed in a mortar. The powder was annealed for 4 h at 700 °C in an oven to give yellow-orange perovskite grains.

2.3. Composite slurry preparation

Sol concentration and powder content were selected after a preliminary study. In this study, the composite slurry was produced by mixing PZT sols of 0.7 M in concentration and PZT powders with powder content (charge load) of 50 wt% (cf. Fig. 1). The mixture was stirred under constant agitation for up to three months to study sol ageing.

2.4. Composite layer deposition and infiltration

Deposition of the composite layer was performed by dip coating on $Si/SiO_2/Ti/Pt$ (1 0 0) and (1 1 1) wafers (6 cm × 3 cm). The substrates were cleaned with optical detergent and washed with distilled water and ethanol prior to coating. In this study, powders were only crushed in a mortar before mixing. The composite solution was then aged under constant agitation to disperse the rough powder in the slurry. Depending on the slurry age, single composite layers can be prepared in the 1–10 μm thickness range. The composite sol was stirred between each deposition step and was calmed during coating. In this study, infiltration was only processed on the whole stack. After coating each layer (composite or infiltration), calcination and densification were performed on a hotplate at 370 °C for 5 min. The composite

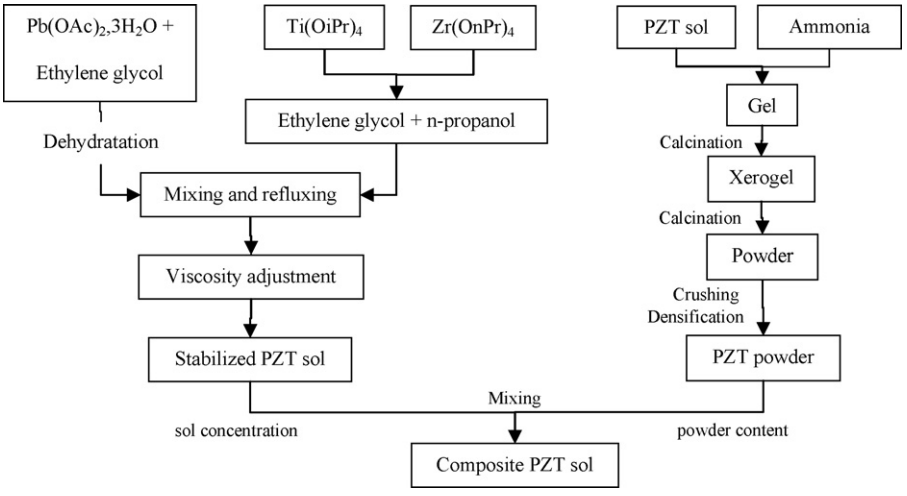

Fig. 1. Composite PZT sol synthesis.

stack was heated for 2 min at 600 °C on a hotplate before infiltration. Films were finally annealed at 700 °C in a furnace or a rapid thermal annealing (RTA) oven. Before poling, 400 nm thick aluminium electrodes were sputter-deposited through a mask. All films were poled in an oil bath at 170 °C for 5 min under 15 V/μm.

2.5. Structural and electromechanical characterisations

Film thickness and roughness were measured with a Dektak ST8 profilometer. The microstructure was observed by cross-sectional optical micrography and scanning electron microscopy (SEM). Apparent porosity was deduced from these micrographs. X-Ray diffraction was used to determine the crystalline structure of the film. Data were collected on an INEL G3000 diffractometer with Cu Kα1 radiation (λ = 1.54178 Å).

Electrical, acoustic and electromechanical parameters of the thickness mode were deduced using a method based on measurement of the complex electrical impedance according to frequency $Z_e(f)$ around the fundamental thickness-mode resonance. The experimental set-up was composed of an HP4395 spectrum analyser with its impedance test kit and specific spring clip fixture. An equivalent electrical circuit scheme was used, the KLM model,[17] for the corresponding modelling. This one-dimensional model is based on the same assumption as Mason's model[18] and allows clear separation of the network of acoustic and electrical ports of the piezoelectric element. Moreover, a matrix formula[19] makes numerical calculation of the multilayer structure integrating a piezoelectric layer easier. The diameter of the top electrode used in this study was large in comparison with the film thickness so that samples only delivered a thickness mode vibration. The thickness of the silicon substrate was also much smaller than its lateral dimension to avoid lateral mode excitation.[20,21] The complex electrical impedance of the multilayer structure can be simulated with the KLM electrical circuit. For our samples, the thickness of the silicon substrate was in the same range as the ratio of longitudinal wave velocity in this substrate and the fundamental resonance frequency of the piezoelectric thick film (assumed in free resonator conditions). The resonances in the silicon substrate were therefore coupled with those in the piezoelectric thick film.[21]

In contrast to the characterisation of a free unbacked resonator,[22] the surrounding layers of similar thickness to that of the piezoelectric thick film (e.g. substrate) must be taken into account. Consequently, if high accuracy of piezoelectric thick film parameters is desired, the properties of the other layers must be precisely known. [1 0 0] and [1 1 1] textured silicon substrates were used. Velocities in [1 0 0] and [1 1 1] directions were deduced from elastic constants and density measurements.[23] The attenuation values in silicon are low and slightly dispersive. In the 20–100 MHz frequency range, the attenuation measured was between 0.03 and 0.043 dB/mm/MHz.[24] A 1.2 μm thick SiO_2 layer was on the upper surface of the silicon susbstrate.[25] The bottom Pt and top Al electrodes had a thickness of 120 and 400 nm, respectively. Attenuation in both electrodes and SiO_2 layers was ignored. Fig. 2 shows the schematic drawing of the multilayer structure and Table 1 summarises all the data of the inert layers in the structure.

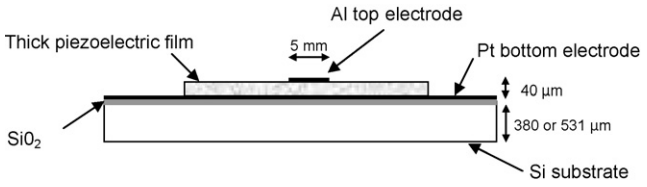

Fig. 2. Schematic drawing (cross-section) of fabricated and characterised samples.

The unknown parameters for the piezoelectric thick film in the KLM model are the effective thickness coupling factor (k_t), the dielectric constant at constant strain (ε_{33}^S), the equivalent longitudinal wave velocity (c_l),[26] and the mechanical and dielectric losses (δ_m and δ_e) measured at the anti-resonance frequency (which are taken into account in the KLM model[27]). These values are obtained with a curve fitting approach by using the simplex method[28] in which effective values are obtained as if the piezoelectric element is loaded with a backing in an ultrasound transducer corresponding to real conditions. Fig. 3 shows the experimental and fitted theoretical complex electrical impedance of the CF1 sample. Good agreement was obtained between theory and experiments.

The influence of variations in several parameters of the inert layers (attenuation, thickness and velocity) on deduced thick piezoelectric film properties was studied. For this, several fits of the first sample characterised (CF1, Table 2) were performed by varying these parameters. The results showed that the attenuation range in the Si substrate given in Table 1 involved only a slight variation in the mechanical losses (around 1%). A variation in thickness or velocity in the Si substrate can significantly change the effective velocity in the piezoelectric thick film but these values in the single Si crystal are known very accurately (Table 1). Simulations were also performed

Table 1
Material properties of inert layers in the structure (t: thickness, c_l: longitudinal wave velocity, ρ: density, Z: acoustic impedance, α: attenuation coefficient, with frequency range study for the substrate)

Layer	Materials	t (μm)	c_l (m/s)	ρ (kg/m^3)	Z (MRa)	α (dB/mm/MHz)
Top electrode	Aluminium	0.4	6320	2700	17.1	–
SiO_2	SiO_2	1.2	5995	2200	13.2	–
Bottom electrode	Platinum	0.12	3960	21400	84.7	–
Substrate	Silicon [1 0 0]	380	8430	2340	19.7	0.03–0.043
	Silicon [1 1 1]	531	9340	2340	21.9	0.03–0.043

Table 2
Properties of films CF1 to CF6 (l: number of infiltrations; [Si]: Silicon substrate crystallographic orientation; e: film thickness; d: diameter of the circular top electrode, P: film porosity; $\varepsilon_{33}^{S}/\varepsilon_0$: dielectric constant at constant strain; k_t: effective thickness coupling factor; δ_m: mechanical losses measured at f_a; e_{33}: piezoelectric coefficient; c_{33}^{E}: elastic constant at constant electric field; f_a: anti-resonance frequency)

Films	l	[Si]	Heating	Annealing time	e (μm)	d (mm)	P (%)	$\varepsilon_{33}^{S}/\varepsilon_0$	k_t (%)	δ_m (%)	e_{33} (C/m^2)	c_{33}^{E} (10^{10} N/m^2)	f_a (MHz)
CF1	12	[1 0 0]	Furnace	4 h	46 ± 2	5.2 ± 0.3	16 ± 5	385 ± 60	33 ± 1.5	7 ± 1	5.6 ± 0.8	7.9 ± 1.4	39 ± 1.5
CF2	4 × 3	[1 0 0]	Furnace	4 h	36 ± 2	5.2 ± 0.3	13 ± 5	340 ± 55	29 ± 1	14 ± 2	4.3 ± 0.7	6.5 ± 1.2	44.5 ± 1
CF3	10	[1 1 1]	Furnace	4 h	40 ± 2	5.3 ± 0.3	11 ± 5	415 ± 60	27 ± 1	14 ± 2	4.6 ± 0.9	6.8 ± 1.3	40.5 ± 1
CF4	10	[1 1 1]	Furnace	10 min	41 ± 2	5.2 ± 0.3	41 ± 5	320 ± 50	36 ± 1.5	14 ± 2	4.2 ± 0.6	4.0 ± 0.7	32 ± 1
CF5	10	[1 1 1]	RTA	10 min	42 ± 2	5.3 ± 0.3	10 ± 5	360 ± 60	36 ± 1	16 ± 2	5 ± 0.7	4.9 ± 0.9	34 ± 1
CF6	5	[1 1 1]	RTA	10 min	40 ± 2	5.2 ± 0.3	17 ± 5	340 ± 40	39 ± 1	15 ± 2	4.5 ± 0.8	3.5 ± 0.7	30.5 ± 1

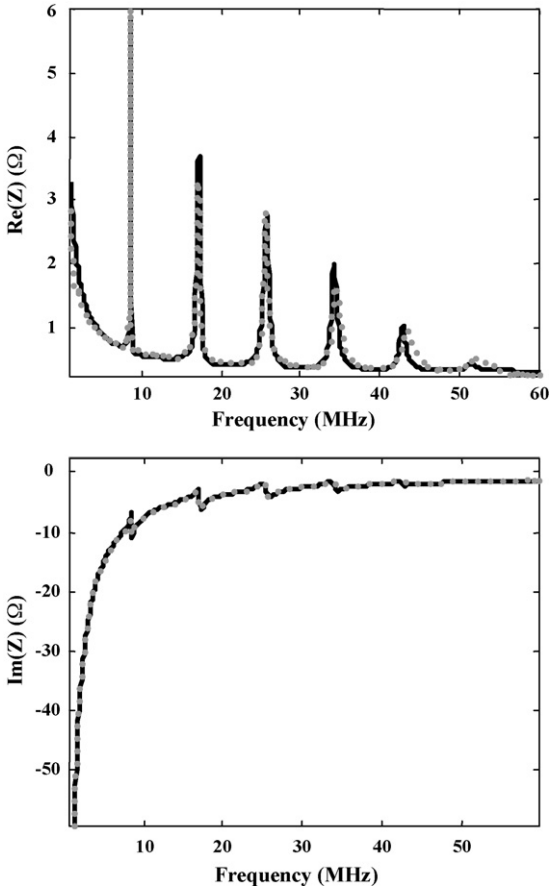

Fig. 3. Electrical impedance of CF1 (solid line: experimental; dashed line: theoretical).

ignoring the SiO_2 layer. The results showed very low variations in the thick film parameters. The absolute variations were around 0.2% and 10 m/s for the effective thickness coupling factor and the longitudinal wave velocity, respectively. Platinum acoustic impedance is high in comparison with that of the thick piezoelectric film (which increases the loaded effect). However, the two electrodes were also very less thick in comparison with the piezoelectric element. As a consequence, these two layers can be ignored (the maximum variation for the five extracted parameters in the piezoelectric thick film was around 0.1%). For the same reason the Ti layer (<50 nm) was also ignored.

3. Results and discussion

3.1. General characterisations

To determine the PZT bulk properties, 10 mm diameter, 500 μm thick pellets were pressed and sintered at 1260 °C. Pt electrodes of about 5 μm thick were screen printed before poling at 130 °C for 2 min under 1.9 V/μm. The pellet exhibited a thickness coupling factor, k_t, of about 50% at 4.1 MHz. This value was as high as those obtained for powders made by the mixed oxide conventional process and shows that this powder is suitable for the preparation of high performance thick films. The

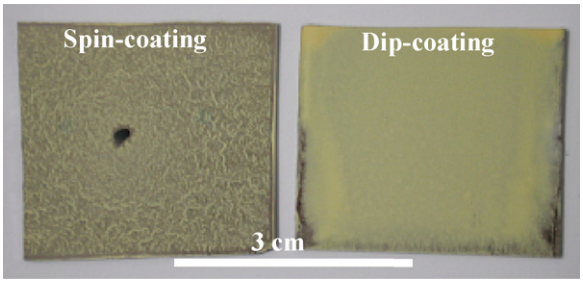

Fig. 4. Photographs of a spin-coated and dip-coated composite single layer.

measured density of the pellets was around 7000 kg/m^3 which confirms a residual porosity.

Films were first deposited by spin coating and dip coating. Both techniques have the advantage of short process time and low volume for spin, and the possibility of depositing on complex shapes and high surface substrate for dip coating. However, as shown in Fig. 4, composite single layers prepared with coarse powder and deposited by spin coating (1000 rpm, 30 s) are less homogeneous compared to dip coating.

A composite PZT film deposited by dip coating was analysed by X-Ray diffraction as shown in Fig. 5. The XRD pattern matches the typical perovskite structure of $PbZr_{0.52}Ti_{0.48}O_3$ (JCPDS Card No. 33-0784). In fact, because PZT with a morphotropic phase boundary (MPB) was studied, rhombohedric and tetragonal structure can coexist. This is shown by the asymmetric profiles of the peaks which indicate that the composition varies locally. As a consequence, the widths of the XRD peaks are meaningless here. Moreover, no lead oxide was detected as a separate phase.

Fig. 6 shows the thickness/layer versus the 50 wt% charged sol ageing. Thickness/layer increased from 3 to 10 μm after 3 months, demonstrating the dispersion of powders described in the literature.[29] These results showed that a wide range of film thicknesses can be easily achieved by composite sol dispersion.

The influence and possible variations (related to possible error measurements) in three experimental parameters on the piezoelectric thick film properties was also studied (i.e. thickness, density and surface area of the top electrode). Variations of ±2 μm in the thickness, ±10% in the area of the top electrode (corresponding to a variation of ±0.3 mm in the diameter) and

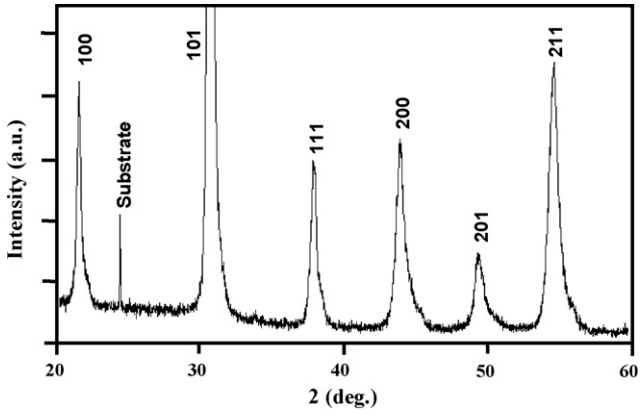

Fig. 5. X-Ray diffraction pattern of a composite thick PZT film.

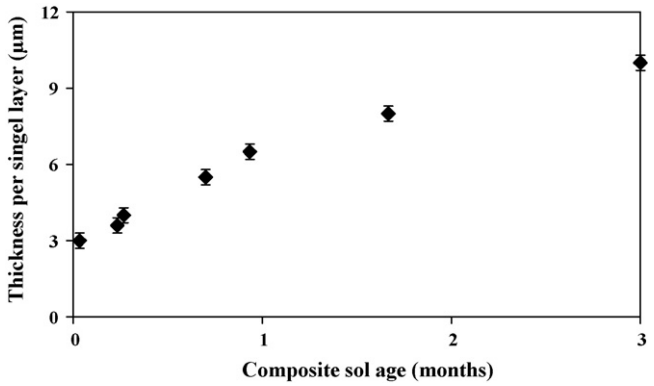

Fig. 6. Single layer thicknesses influence by sol ageing.

7–25% of porosity in the film (corresponding to a density range between 6000 and 7440 kg/m^3) were taken into account for the determination of five parameters by the fitting process: dielectric constant at constant strain, thickness coupling factor, longitudinal wave velocity, mechanical losses and electrical losses. Corresponding ranges of variation were quantified for each of these parameters; elastic constant (c_{33}^{E}), piezoelectric coefficient (e_{33}) and anti-resonance frequency (f_a) were deduced. All the results are summarised in Table 2. The dielectric losses were between 1 and 2% for all samples.

The results showed that variations in effective thickness coupling coefficients did not exceed ±0.015. Accuracy of longitudinal wave velocity was also less than 5%. In contrast, dielectric constant at constant strain and mechanical losses varied between 10 and 15%.

Effective thickness coupling coefficients were high although piezoelectric coefficients (e_{33}) were low compared to other reports. This can be mainly explained by the very low values of dielectric constant that counterbalance the low e_{33}. This result was previously reported by Lukacs et al.[20]

3.2. Influence of intermediate and final infiltrations

To compare intermediate and final infiltrations, two films (CF1 and CF2) were prepared with a composite solution aged for 3 months. CF1 was made with 3 composite layers and 12 final infiltrations. CF2 was deposited using 3 composite layers and 4 intermediate infiltrations/layer, also leading to 12 infiltrations. CF1 (46 μm) was thicker than CF2 (33 μm). In fact, the first infiltrations probably create barrier layers. As a consequence, the last infiltration layers in CF1 slightly increased the film thickness.

Few infiltrations were required to pole the films here to prevent voltage break down. Poling and piezoelectric measurements were performed on these composite layers as described in Sections 2.4 and 2.5. CF1 exhibited an effective thickness coupling factor of 33% at 39 MHz (Table 2). This value was quite low compared to the bulk properties but higher than that of CF2. The slight difference between CF1 and CF2 can be explained by the microstructure at the film/substrate interface.[30] Indeed, the adhesion of the film on the substrate was lower in CF1 than in CF2, as seen in Fig. 7, as its interface was more porous.

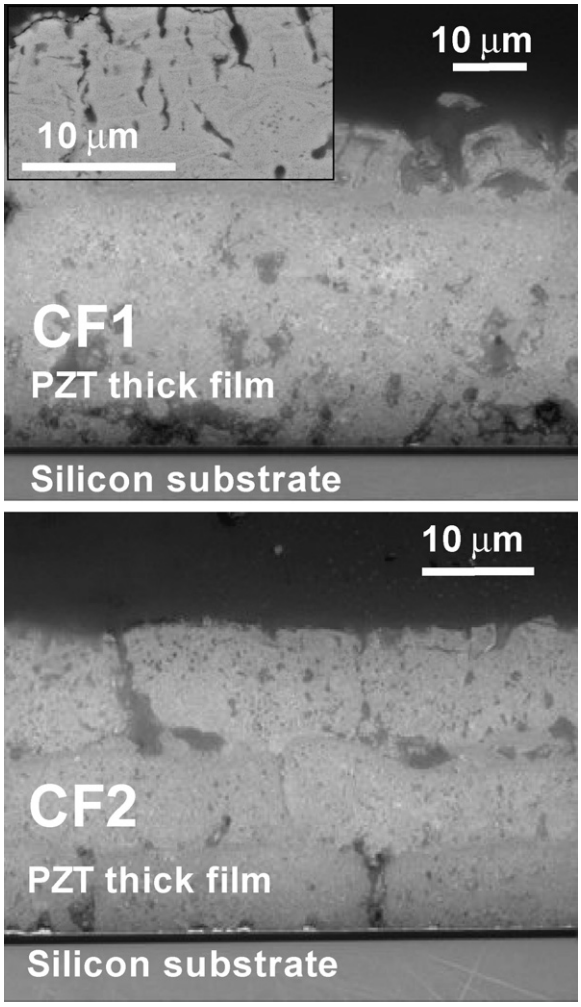

Fig. 7. Cross-section SEM micrographs of CF1 and CF2.

3.3. Influence of heat treatment process and duration

Various heat treatments were processed on further films prepared with 2-month-old slurry (Table 2). The thermal curing was the same as for CF1 and CF2 except the final annealing. To reach the 40 μm thickness, 6-layered composite stacks and 10 final infiltrations were deposited. Table 2 shows that short annealing time duration allowed the preparation of good performance layers. For instance, an up to 36% effective coupling coefficient k_t was obtained at 34 MHz for 10 min rapid thermal annealing at 700 °C. This result is very close to the best value already reported by Sayer et al.[11] Longer time duration heat treatment leads to non-reproducible performance, e.g. CF1 and CF3, depending on the film densification and mechanical stresses induced. It can also modify the film/substrate interface where atom diffusion takes place. High mechanical losses in the 3 films may be due to inhomogeneous porosity distribution or thickness variations in the films.

3.4. Influence of the number of infiltrations

A new film (CF6) was prepared with the same process as for CF5 but with only 5 final infiltrations. Film electromechanical properties are reported in Table 2. An effective coupling coefficient k_t of 39% at 30 MHz was then obtained which was better than for CF5, although CF6 was more porous than CF5. The dielectric constant $\varepsilon_{33}^{S}/\varepsilon_0$ was therefore lower in CF6 than in CF5, leading to an increase in k_t. This result shows that adding more infiltrations improves film density but not piezoelectric performance. In conclusion, this study shows that a minimum number of final infiltrations is appropriate for composite sol–gel processes and can lead to high piezoelectric properties.

4. Conclusion

Thick piezoelectric PZT films were made by dip coating of a composite sol–gel solution followed by polymeric sol infiltration. The composite mixture was prepared with a very stable diol-based PZT precursor sol and PZT powder made from the same solution. By varying the final annealing, the infiltration process and the number of infiltrations, effective electromechanical coupling coefficient of up to 39% at a resonance frequency of 30 MHz, suitable for high frequency transducer applications, can be reached on a platinised silicon wafer. This study shows that high piezoelectric properties in the right frequency range can be achieved with a limited number of layers, thus saving time and cost. Moreover, a final infiltration process seems to yield better piezoelectric results than an intermediate process. Furthermore, the dip-coating process allows the deposition of thick film on a dome shaped substrate. The influence of particle size and single layer thickness is currently under investigation, and other substrates more suitable for ultrasound transducers will also be studied.

Acknowledgements

The authors wish to thank E. Estrade for microscopy analysis, S. Lambert for XRD and E. Ringgaard from Ferroperm Piezoceramics A/S (Denmark) for bulk ceramic fabrication (powder sintering and ceramic poling).

The study was supported by the Commissariat à l'Energie Atomique (CEA) and the Region Centre in France.

References

1. Lockwood, G. R., Turnbull, D. H. and Foster, F. S., *Transactions on Ultrasonics, Ferroelectrics and Frequency Control*, 1994, **41**, 231–235.
2. Levassort, F., Tran-Huu-Hue, L. P., Lethiecq, M., Bove, T. and Wolny, W., *IEEE International Ultrasonics Symposium*, 2001, 1125–1128.
3. Tran-Huu-Hue, L. P., Levassort, F., Meulen, F. V., Holc, J., Kosec, M. and Lethiecq, M., *Journal of the European Ceramic Society*, 2001, **21**, 1445–1449.
4. Barrow, D. A., Petroff, T. E. and Sayer, M., *Surface and Coatings Technology*, 1995, **76–77**, 113–118.
5. Noguera, R., Lejeune, M. and Charetier, T., *Journal of the European Ceramic Society*, 2005, **25**, 2055–2059.
6. Fukushima, J., Kodeira, K. and Matsuhita, T., *Journal of Materials Science*, 1984, **19**, 595.
7. Tsurumi, T., Num, S. M., Kil, Y. B. and Wada, S., *Ferroelectrics*, 2001, **259**, 43.
8. Waser, R., Schneller, T., Ehrhart, P. and Hoffman-Eifert, S., *Ferroelectrics*, 2001, **259**, 205.

9. Schroth, A., Lee, C., Matsumoto, S. and Maeda, R., *Sensors and Actuators*, 1999, **144**.
10. Barrow, D. A., Petroff, T. E., Tandon, R. P. and Sayer, M., *Journal of Applied Physics*, 1997, **81**, 876–881.
11. Sayer, M., Lukacs, M., Olding, T., Pang, G., Zou, L. and Chen, Y., *Materials Research Society Symposium Proceeding*, 1999, 541.
12. Corker, D. L., Zhang, Q., Whatmore, R. W. and Perrin, C., *Journal of the European Ceramic Society*, 2002, **22**, 383–390.
13. Dorey, R. A. and Whatmore, R. W., *Integrated Ferroelectrics*, 2002, **50**, 111–119.
14. Dorey, R. A., Haigh, R. D., Stringfellow, S. B. and Whatmore, R. W., *British Ceramic Transactions*, 2002, **101**, 146–148.
15. Belleville, P., Boy, P. and Montouillout, Y., WO 03/024871, 2003.
16. Ohya, Y., Itoda, S., Ban, T. and Takahashi, Y., *Journal of Applied Physics*, 2002, **41**, 270–274.
17. Leedom, D. A., Kimholtz, R. and Matthaei, G. L., *Transactions on Sonics and Ultrasonics*, 1971, **18**.
18. Kino, G. S., *Acoustic Waves: Devices, Imaging, and Analog Signal Processing*. Prentice-Hall, New Jersey, 1987.
19. Van Kervel, S. J. H. and Thijissen, J. M., *Ultrasonics*, 1983, **21**, 134–140.
20. Lukacs, M., Sayer, M. and Foster, S., *Ferroelectrics*, 2000, **47**, 148–159.
21. Lukacs, M., Olding, T., Sayer, M., Tasker, R. and Sherrit, S., *Journal of Applied Physics*, 1999, **85**, 2835–2843.
22. ANSI/IEEE standard 176, 1987.
23. Royer, D. and Dieulesaint, E., *Propagation libre et guidée*. Masson, 1996.
24. Martin, E., Thesis. Joseph Fourier University, 2007.
25. Duval, F. F. C., Dorey, R. A., Wright, R. W., Huang, Z. and Whatmore, R. W., *Ferroelectrics*, 2004, **51**, 1255–1261.
26. Maréchal, P., Levassort, F., Holc, J., Tran-Huu-Hue, L. P., Kosec, M. and Lethiecq, M., *IEEE Transactions on Ultrasonics, Ferroelectrics, and Frequency Control*, 2006, **53**, 1524–1533.
27. Lethiecq, M., Tran-Huu-Hue, L. P., Patat, F. and Pourcelot, L., *IEEE Transactions on Ultrasonics, Ferroelectrics, and Frequency Control*, 1993, **40**, 232–237.
28. Lagarias, J. C., Reeds, J. A., Wright, M. H. and Wright, P. E., *SIAM Journal on Control and Optimization*, 1998, **9**, 112–147.
29. Randall, M. G., *Powder Injection Modeling*. Metal Powder Industries Federation, Princeton, New Jersey, 1990.
30. Barzegar, A., Damjanovic, D. and Setter, N., *IEEE Transactions on Ultrasonics, Ferroelectrics, and Frequency Control*, 2004, **51**, 262–270.